

Article

Is *ortho*-Cresol a Viable Lignocellulosic Blendstock? A Kinetic Study of Its Co-Oxidation within a Surrogate Fuel

 Carolina S. Mergulhão, Yann Fenard  and Guillaume Vanhove * 

Université Lille, CNRS, UMR 8522-PC2A-Physicochimie des Processus de Combustion et de l'Atmosphère, F-59000 Lille, France; carol.mergulhao@hotmail.com (C.S.M.); yann.fenard@univ-lille.fr (Y.F.)

* Correspondence: guillaume.vanhove@univ-lille.fr; Tel.: +33-3-20-43-44-85

Abstract: The viability of the use of *ortho*-cresol as a bio-blendstock or antiknock additive from lignocellulosic biomass is assessed; Ignition delays of *ortho*-cresol within blends with *iso*-octane are measured with the ULille rapid compression machine, and compared with results from the literature; It is shown that *ortho*-cresol has a strong inhibiting effect on the reactivity towards ignition, most notably in the Negative Temperature Coefficient region; This effect is found to originate from competition with *iso*-octane on the OH radicals, where the reactivity of *ortho*-cresol with these radicals does not lead to radical chain-branching.

Keywords: ignition delay; low-temperature combustion; *ortho*-cresol; co-oxidation; kinetic modeling; rapid compression machine; surrogate fuel



Citation: Mergulhão, C.S.; Fenard, Y.; Vanhove, G. Is *ortho*-Cresol a Viable Lignocellulosic Blendstock? A Kinetic Study of Its Co-Oxidation within a Surrogate Fuel. *Energies* **2021**, *14*, 7105. <https://doi.org/10.3390/en14217105>

Academic Editor: Goutham Kukkadapu

Received: 29 September 2021

Accepted: 20 October 2021

Published: 1 November 2021

Publisher's Note: MDPI stays neutral with regard to jurisdictional claims in published maps and institutional affiliations.



Copyright: © 2021 by the authors. Licensee MDPI, Basel, Switzerland. This article is an open access article distributed under the terms and conditions of the Creative Commons Attribution (CC BY) license (<https://creativecommons.org/licenses/by/4.0/>).

1. Introduction

The quest for viable and affordable bio-blendstocks has led researchers to explore the potential of lignin-based compounds for the production of alternative fuels. Such alternative fuels have strong requirements for compliance with existing spark-ignition engine technologies, among which sufficient resistance to engine knock. Knock is caused by unwanted auto-ignition of the fuel/air mixture and is commonly evaluated by octane number measurements. Lignin is a cheap source of species in the structure of which the presence of an aromatic ring is often viewed as a guarantee of strong anti-knock behavior. Among such species, *ortho*-cresol has been identified as a promising additive in a kinetic modeling study aiming at comparing the anti-knock tendencies of various oxygenated aromatics [1]. This effect was discussed and suggested to originate from the relative stability of 2-methylene, cyclohexa-3,5-dien-1-one, a species that can be formed easily from the two most expected radicals in the case of *ortho*-cresol. These two radicals, later referred to as R1 and R2, are presented in Figure 1 along with the structure of *ortho*-cresol. Both of them are stabilized by resonance, and can therefore be long-lived in reactive systems, and difficultly undergo chemical chain-branching. It is also possible that such radicals recombine with the HO₂ radical, thereby forming an unstable hydroperoxide, as observed for alkenes [2,3] or the benzyl radical [4]. These pathways have however not been considered in [1]. Blending experiments within a diesel fuel have also demonstrated a reduction in NO_x and soot emissions from a compression-ignition engine when *ortho*-cresol is added [5].

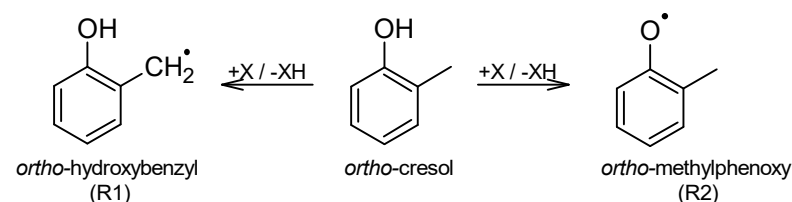


Figure 1. The structure of *ortho*-cresol and its most expected radicals in the low-temperature combustion domain: *ortho*-hydroxybenzyl (R1) and *ortho*-methylphenoxy (R2).

ortho-cresol is also a very common product of the oxidation of aromatics [4,6] in combustion applications, as well as of the pyrolysis of biomass [7–9]. There is however a lack of available literature on its combustion kinetics. Moreover, in practical conditions, *ortho*-cresol can be in presence of a radical pool that may not exist if it had been on its own. Especially, in the case of automotive fuels, species that are often considered unreactive can undergo co-oxidation because of the presence of a more reactive compound inside the fuel blend. Studying co-oxidation conditions is therefore of crucial importance in order to include all the necessary pathways into kinetic models, as demonstrated in the past [4,10–12]. To serve that purpose, because of its two-stage ignition features and relevance to spark-ignition engine fuels, *iso*-octane was used as a co-oxidant in this study.

Therefore, the present study aims at evaluating the potential of *ortho*-cresol as a bio-blendstock, and gaining insight into the low-temperature oxidation pathways of *ortho*-cresol at high pressures, through an experimental study of the ignition of isooctane/*ortho*-cresol blends inside a rapid compression machine (RCM). The obtained results will be compared with those from a model available in the literature, after which this model will be used to gain insight into the results and the effect of *ortho*-cresol on the ignition delays of *iso*-octane. To the authors' knowledge, this constitutes the first experimental study of the combustion kinetics of *ortho*-cresol.

2. Materials and Methods

2.1. Experimental Methods

The ULille RCM was used to measure the ignition delays of stoichiometric *iso*-octane/*ortho*-cresol blends at several blending ratios between 0 and 40% mol. *ortho*-cresol in the fuel blend, and at pressures between 14 and 20 bar, and temperatures between 688 and 850 K. Because this experimental setup has been described extensively in the literature before [11–13], a schematic being given in [14], only the features relevant to this work will be described here. Mixtures of *iso*-octane, *ortho*-cresol, dioxygen, and inert gases were prepared using the partial pressure method inside a heated mixture preparation facility, whose temperature was fixed as superior to the one necessary for a vapor pressure of all compounds superior to twice the required one. All lines leading to the RCM were heated to a temperature superior by 5 K to this temperature to prevent any condensation. The temperature at top dead center was calculated from the adiabatic core assumption and varied by using a mixture of diluents including CO₂, N₂, and Ar. The composition of the mixtures used in this study is given in the Supplementary Material.

First-Stage (FSIDT) and total Ignition Delay Times (IDT) are defined as the time lapse between the Top Dead Center (TDC) and their respective maximum in pressure derivative. A creviced piston and a reproducible compression time of 45 ms were used to prevent the formation of a piston corner vortex during compression. During the modeling of the results, volume profiles processed from experiments where O₂ was replaced by N₂ were used as input to model the compression phase and the heat losses after compression. These volume profiles are also provided as Supplementary Material. An uncertainty of ±5 K and ±0.1 bar is assumed on the reported temperatures and pressures, respectively. All of the measured IDTs are reported in the figures, demonstrating the reproducibility of the measurement.

2.2. Kinetic Modeling

All simulations were performed using the Cantera solver [15]. The model used in this work is a kinetic model for the oxidation of anisole–isooctane blends [11]. The submechanism describing the oxidation of *iso*-octane originates from the work by Fang et al. [16]. The anisole submechanism was updated from a model by Wagnon et al. [17] on the basis of new ab initio calculations. It contains a submechanism for the combustion kinetics of cresol sharing large similarities with the submechanism proposed by Bounaceur et al. [18]. To the authors' knowledge, detailed kinetic models dealing with the oxidation of cresols are scarce in the literature and have not been the subject of dedicated studies.

In the early 1990s, Emdee et al. [19] observed the formation of cresols during the oxidation of toluene in a flow reactor. They explained their kinetics of formation by an electrophilic addition of an O atom on the aromatic ring by toluene + O = cresoxy + H or the addition of a methyl radical on phenol giving cresol and an H-atom. The cresoxy radical can further recombine with an H atom to form cresol. Lindstedt et al. [20] refined this model by considering the consumption of cresols via H loss and H-atom abstraction by H and OH at the hydroxyl position followed by the decomposition of the cresoxy radical yielding benzene, CO, and an H-atom. The mole fraction profiles of toluene oxidation products were measured in a JSR (Jet-Stirred Reactor) and the ignition delay times of toluene/oxygen/argon mixtures were measured in a shock tube [18]. The authors developed a detailed kinetic model reproducing their experimental data. This model contains primary and secondary mechanisms of the oxidation of toluene, and among them, a sub-mechanism for the oxidation of cresols and derived radicals. The H-atom abstraction reactions forming two different radicals were considered. The reaction rate parameters for the formation of the methylphenoxyl radical ($I < 3500 \text{ wonOC}_6\text{H}_4\text{CH}_3$) were taken equal to phenol [21] and for the formation of hydroxylbenzyl radical ($\text{HOC}_6\text{H}_4\text{CH}_2$) were taken equal to toluene [18]. The consumption of methylphenoxyl radicals happens via CO elimination to form the methycyclopentadienyl radical, when the consumption of hydroxylbenzyl radicals occurs by additions to molecular oxygen or to the hydroperoxyl radical. These two last reactions mainly lead to the formation of methylbenzaldehyde. It can be noted that none of these models consider the *ortho*-, *meta*-, or *para*- structure of the cresol isomers, which are lumped into one species.

3. Results

3.1. Ignition Delays

The effect of the addition of *ortho*-cresol on the ignition delays of *iso*-octane/*ortho*-cresol blends is displayed in Figure 2 at two different compressed temperatures $T_C = 686$ and 850 K. At $T_C = 686$ K, the mixture displays two-stage ignition, representative of the transition from low-temperature to intermediate-temperature combustion. As the *ortho*-cresol fraction increases, both first-stage and total ignition delay increase monotonically. Both ignition delays are simulated with an acceptable agreement in this condition, with a maximum deviation of about 30%. This discrepancy is nearly constant, and also observable in the pure *iso*-octane case. This suggests that in these conditions, the effect of *ortho*-cresol addition is well captured by the model. However, at $T_C = 850$ K, the experiments show little to no effect of *ortho*-cresol addition on the ignition delays, while the model predicts a large increase in the IDT. Note that no first-stage ignition was observed at this higher temperature, in agreement with similar studies with *iso*-octane [14]. This is consistent with the reduced performance of the model in this temperature range in the case of *iso*-octane/*anisole* blends, as observed in [11].

These conclusions can be generalized over a wide range of pressures, as demonstrated in Figure 3. The discrepancy between experimental and simulated ignition delays is consistent all over the investigated pressure range for pure *iso*-octane mixtures, with an underestimation of the IDT of about 30% at $T_C = 850$ K, and a similar overestimation of both IDTs at $T_C = 686$ K. While this remains true at all investigated *ortho*-cresol mole fractions for the lowest temperature, where two-stage ignition is observed, the model again overestimates the effect of *ortho*-cresol addition on the IDT at all pressures. Experimentally, the addition of *ortho*-cresol hardly modifies the IDT at $T_C = 850$ K.

To gain further insight, an 80/20% mol. *iso*-octane/*ortho*-cresol mixture was further studied. A comparison of the evolution of its IDTs as a function of temperature with a pure *iso*-octane case is pictured in Figure 4. Both cases demonstrate Negative Temperature Coefficient (NTC) behavior, but the temperature domain at which this behavior is observed is however shorter for the mixture case in comparison to pure *iso*-octane. *Ortho*-cresol addition results in an increase in the IDT at all investigated temperatures, this effect being maximal in the NTC zone. Around 750 K, the IDTs are multiplied by about a factor of 6 by

blending 20% of *ortho*-cresol into *iso*-octane. The temperature range at which first-stage ignition could be observed is also shorter than in the case of pure *iso*-octane, for which first-stage ignition is still observed for T_C above 750 K. However, at the highest investigated temperature $T_C = 850$ K, the effect of *ortho*-cresol addition is nearly negligible, as discussed above. The model captures the increase in the IDT and reproduces the experimental first-stage and total IDTs with a fair agreement for the pure *iso*-octane and blend cases, especially considering that it was not validated on experimental data on *ortho*-cresol before, and was not modified as part of this study. Additional work on the accurate reproduction of the ignition chemistry of *iso*-octane in the NTC temperature range could help improve these results.

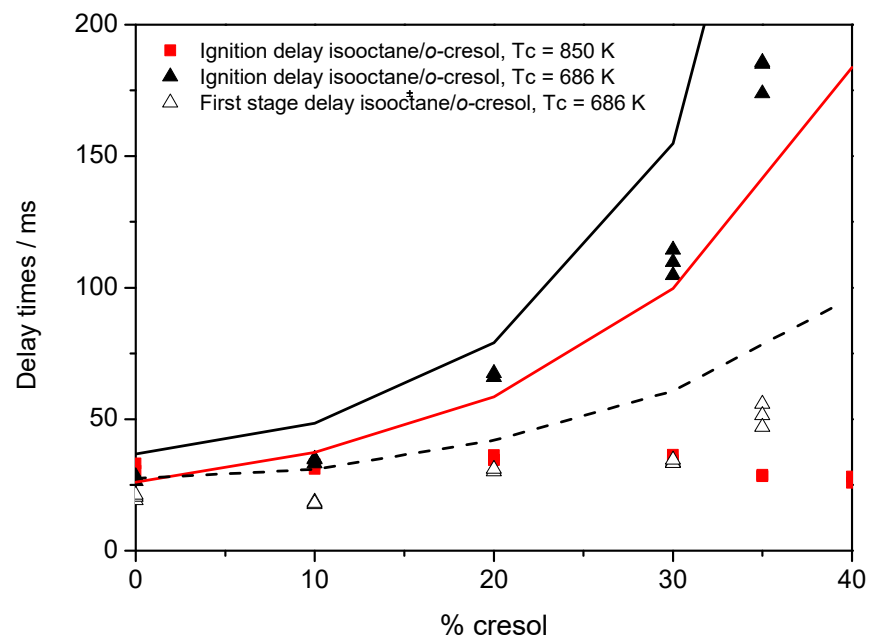


Figure 2. Experimental (symbols) and simulated (lines) evolution of the first-stage (open symbols, dashed line) and total (full symbols, solid lines) ignition delay times of stoichiometric *iso*-octane/*ortho*-cresol blends as a function of the molar content in *ortho*-cresol. $T_C = 686 \pm 7$ K (black), 850 ± 5 K (red), $P_C = 20$ bar.

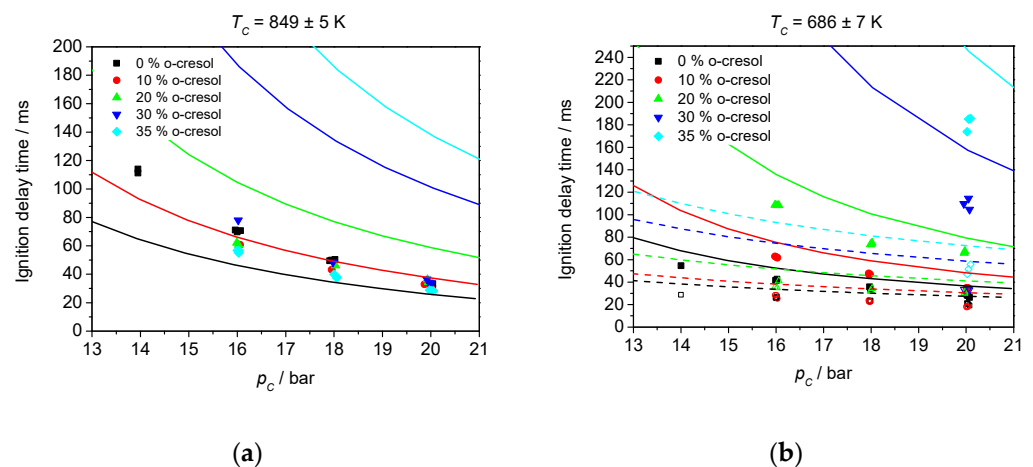


Figure 3. Experimental (symbols) and simulated (lines) effect of the compressed pressure P_C on the first-stage (open symbols, dashed lines) and total (full symbols, solid lines) ignition delays of stoichiometric *iso*-octane/*ortho*-cresol mixtures. (a) $T_C = 850 \pm 5$ K, (b) 686 ± 7 K.

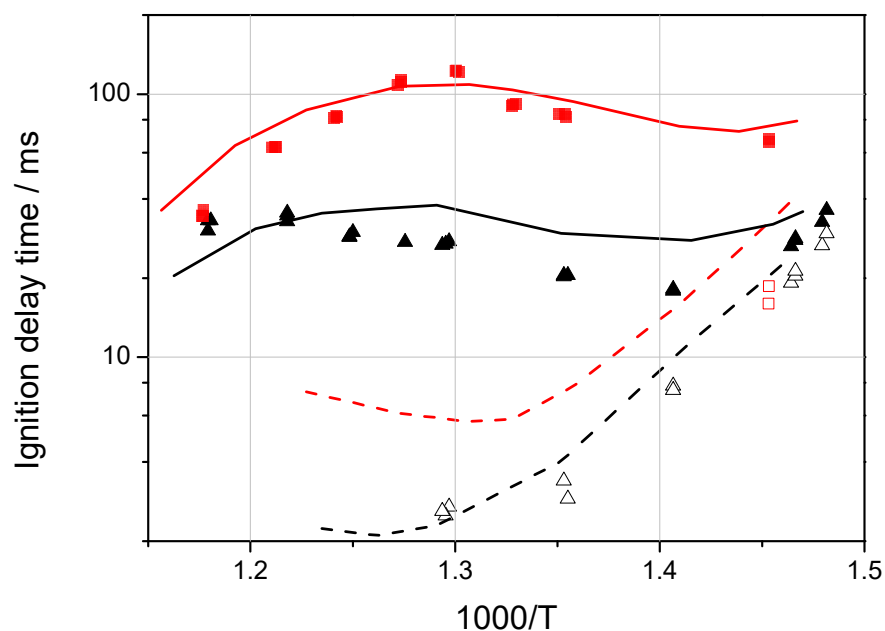


Figure 4. Experimental (symbols) and simulated (lines) evolution of the first-stage (open symbols, dashed lines) and total (full symbols, solid lines) ignition delays for stoichiometric pure *iso*-octane/'air' (black) and 80/20% mol. *iso*-octane-*ortho*-cresol/'air' (red) mixtures with the core gas temperature T_C . $P_C = 20$ bar.

3.2. Kinetic Analysis

Because this study focuses on the co-oxidation of *ortho*-cresol in conditions where it will not show auto-ignition, the following discussion will examine further the $T_C = 686$ K condition, where two-stage ignition takes place. A brute-force sensitivity analysis on the first-stage and total ignition delays has been performed and is shown in Figure 5. Because of the size of the mechanism and the focus on explaining the effect of *ortho*-cresol, this sensitivity analysis was performed only taking into account the submechanism for this species, as well as radicals R1 and R2, phenol, and the phenoxy radical. First, one can note that the two hydrogen abstraction reactions by OH leading to R1 and R2 have the highest sensitivity coefficient for both ignition delays. The fact that both have positive sensitivity coefficients illustrates that *ortho*-cresol acts mainly as a radical scavenger of OH, thereby reducing the reactivity in the low-temperature zone. This is also true for the hydrogen abstraction reaction by OH on *ortho*-hydroxybenzaldehyde, demonstrating the importance of this secondary species, which will be confirmed below. Moreover, the formation of R2 inhibits the reactivity more than the corresponding reaction forming R1. This can be explained by the fact that according to the simulations, R2 is mainly recycled into cresol, when R1 can undergo further reactivity with HO_2 and O_2 . This creates a reactivity loop where R1 then reacts with HO_2 to yield back *ortho*-cresol, and this reaction therefore shows a positive sensitivity coefficient on the first-stage ignition delay. This conclusion can however be toned down by the fact that further reaction pathways for radical R2, such as the ones yielding cyclohexa-3,5-dien-1-one described in [1], are not present in the kinetic model. One can also notice the negative sensitivity coefficient of the HO_2 addition reaction on radical R1. This results in the formation of a hydroperoxide which can readily decompose into a hydroxybenzoy radical and an OH radical, therefore facilitating ignition by converting a relatively unreactive HO_2 radical into more reactive radicals. The hydrogen abstraction reaction by HO_2 that yields R1 however has a negative sensitivity coefficient on the total ignition delay while its sensitivity coefficient for the first-stage ignition delay is nearly equal to zero, showing that during the second stage of ignition (or in the intermediate temperature range) *ortho*-cresol can reduce the ignition

delay by facilitating the conversion of HO_2 into H_2O_2 , whose decomposition into two OH radicals is commonly associated with the final ignition event.

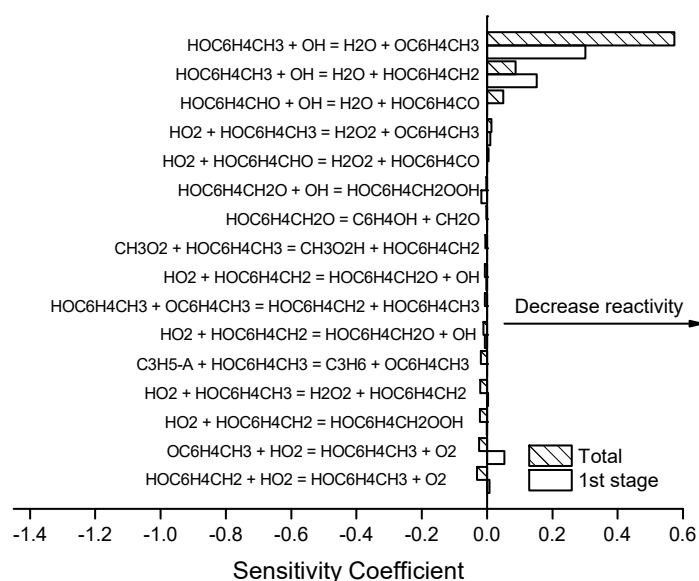


Figure 5. Brute-force sensitivity analysis on the first-stage and total ignition delays of a stoichiometric 80/20 *iso*-octane/*ortho*-cresol mixture. $T_C = 686$ K, $P_C = 20$ bar.

A reaction pathway analysis was also performed to shed light on the main conversion channels of *ortho*-cresol and its products at two stages of the ignition delay of the 80/20 *iso*-octane/*ortho*-cresol blend at $T_C = 686$ K. The first one corresponds to 5% conversion of *ortho*-cresol and the first-stage ignition chemistry, while the second one corresponds to 75% conversion of *ortho*-cresol and the chemistry corresponding to the final ignition stage. The results of this analysis are shown in Figure 6. They show that during the first stage of ignition, R2 is formed preferentially by hydrogen abstraction by OH. However, since none of its conversion pathways are active in these conditions, it easily converts back to *ortho*-cresol, mostly by converting an HO_2 radical into O_2 . This loop is effective in reducing the reactivity of the mixture towards first-stage ignition, by converting two radicals into stable species, but could result from missing reaction pathways, as mentioned above. When R1 is formed, it mainly reacts by recombining with HO_2 , thereby forming a hydroperoxide that decomposes into the *ortho*-hydroxyl-benzyloxy radical, which will in turn form *ortho*-hydroxybenzaldehyde. This compound is also formed minorly by the addition of R1 to O_2 .

During the ignition stage, the conversion of R1 still leads mostly to hydroxy-benzaldehyde. However, the balance between the direct channel of the addition of R1 to HO_2 and the stabilization of the hydroperoxide is shifted towards the former pathway. At all temperatures, *ortho*-hydroxybenzaldehyde reacts through hydrogen abstraction on the carbonylic carbon atom site, and the thereby formed radical undergoes the elimination of carbon monoxide to yield the phenoxy radical. The fate of the phenoxy radical lies in losing a hydrogen atom to form cyclohexadienone isomers, or to abstract a hydrogen atom to yield phenol. At higher temperatures, an alternate pathway leading to CO and the cyclopentadienyl radical is also possible.

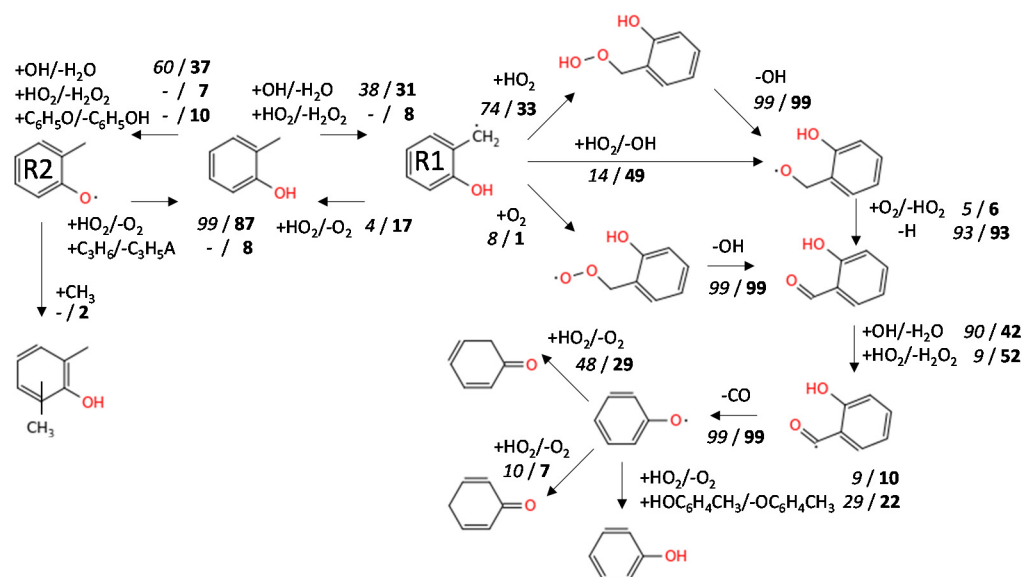


Figure 6. Rate of production analysis for the submechanism of *ortho*-cresol in the case of a stoichiometric 80/20 *iso*-octane/*ortho*-cresol blend at $T_C = 686$ K. $P_C = 20$ bar. Italic numbers correspond to 5% *ortho*-cresol conversion (i.e., first-stage ignition), bold numbers to 75% *ortho*-cresol conversion (i.e., final ignition).

4. Discussion

Insight on the inhibiting effect of *ortho*-cresol can be gained from the kinetic analysis. The inhibiting effect originates from a radical scavenging effect of *ortho*-cresol, which is mainly due to the implication of OH radicals into hydrogen abstraction reactions. OH radicals are typically formed in this case by the active low-temperature branching originating from *iso*-octane which induces first-stage ignition. This scavenging effect results in reduced heat release in the first-stage ignition, thereby limiting the temperature increase and increasing the duration of the second stage of ignition. This results in comparable first-stage ignition delays for blends with up to 30% *ortho*-cresol, as demonstrated in Figure 2, while the total ignition delay increases monotonically as the *ortho*-cresol content increases. When R2 is formed in the first stage of ignition, it does not lead to radical chain-branching since its most important conversion channels require higher temperatures. R1 can undergo further reactivity, but then yields phenol, cyclohexadienones, or *ortho*-hydroxybenzaldehyde, i.e., species which do not contribute to the formation of radicals in significant quantities.

A model developed to describe the co-oxidation of anisole, with an updated phenol and phenoxy submechanism and an *ortho*-cresol submechanism initially developed from toluene studies is able to predict the measured IDTs fairly without further refinement. It therefore constitutes a useful first step for future research on *ortho*-cresol. Despite the fair performance of the model, suggestions on further improvement of the model can be made: First, the model is lumped for all three isomers, but the bond dissociation energies are different for the three cresol isomers, as exemplified for the O–H bonds in *m*-, *p*-, *o*-cresol [22]: *ortho*-cresol = 86.1 < *para*-cresol = 87.2 < phenol = 88.0, *meta*-cresol = 89.4 in kcal/mol. This results in global rate constants for the thermal hydrocracking of cresols decreasing in the order: $k(\textit{ortho}) > k(\textit{para}) > k(\textit{meta})$ [23]. The relative position of methyl and hydroxyl substituents, therefore, has an effect on the reaction rates, especially in the case of H-atom abstraction reactions that lead to the reactivity of *ortho*-cresol, as suggested by the present work in Figure 6. Second, as described above, most reaction rates specific to *ortho*-cresol in the model come from analogies with toluene and phenol and can certainly be refined with help from ab initio calculations. Finally, additional pathways could be added into the model, such as additional reaction pathways for R1 and R2 or H-atom abstractions from the aromatic ring. It is often expected that the H-atom abstraction reactions from an aromatic ring are not competitive with those happening on the substituents, especially in

low-temperature conditions. Nevertheless, this class of reactions was found to be sensitive in the case of anisole [11], especially because of hydrogen bonding facilitating the formation of a pre-complex. Moreover, this work on the co-oxidation of anisole showed possible reaction pathways for the relevant methoxyphenyl radical with molecular oxygen, and their significance for the accurate modeling of the mole fraction profiles of reaction intermediates. These additional improvements of the kinetic model are likely to improve the description of the kinetics of co-oxidation of *ortho*-cresol.

5. Conclusions

In this study, the ignition delay times of *iso*-octane/*ortho*-cresol/air mixtures were measured in the ULille RCM, thereby constituting one of the first experimental studies of the combustion kinetics of *ortho*-cresol. The experimental data are used to check the performances of a model from the literature which has never been validated against the oxidation of *ortho*-cresol. The model is able to predict the FSIDT and IDT of the blends with an acceptable agreement.

ortho-cresol demonstrated an inhibiting effect on the low-temperature combustion oxidation mechanism of *iso*-octane, as evidenced by the experimental results. In the low-temperature range, cresol drastically decreases the reactivity of *iso*-octane/air mixtures even at a low blending ratio. However, in the intermediate temperature range, the IDTs of the blends are mostly similar to those of pure *iso*-octane. This can result in an increase in octane number sensitivity when *ortho*-cresol is blended with *iso*-octane. The conversion of cresol is led by the H-atom abstraction by hydroxyl radicals, acting as a radical scavenger. The resulting fuel radicals can react with HO₂ reforming cresol, therefore, inhibiting the overall reactivity. In conclusion, *ortho*-cresol has a strong anti-knock effect as it strongly increases the ignition delay times when blended with *iso*-octane, however low-temperature reactivity is not fully suppressed. It should also be noted that the fact that the phenoxy radical is easily formed can result in the formation of large quantities of polycyclic aromatic hydrocarbons, as well as their oxygenated counterparts. More fundamental studies, including ab initio calculations of the relevant rate constants, would help gain further insight into the oxidation behavior of cresols.

Supplementary Materials: The following are available online at <https://www.mdpi.com/article/10.3390/en14217105/s1>. Table S1: List of the experimental conditions and IDT values, as well as volume profiles of use for the simulations.

Author Contributions: Investigation, C.S.M.; validation, C.S.M. and G.V.; methodology, Y.F. and G.V.; writing—original draft, G.V.; writing—review and editing, Y.F.; supervision, G.V.; project administration, G.V.; funding acquisition, G.V. All authors have read and agreed to the published version of the manuscript.

Funding: This work is a contribution to the CPER research project CLIMBIO. The authors thank the ADEME, the French Ministère de l'Enseignement Supérieur et de la Recherche, the Hauts-de-France Region and the European Funds for Regional Economical Development for their financial support to this project.

Data Availability Statement: The data presented in this study are available in the Supplementary Material.

Conflicts of Interest: The authors declare no conflict of interest. The funders had no role in the design of the study; in the collection, analyses, or interpretation of data; in the writing of the manuscript, or in the decision to publish the results.

References

1. Zhang, P.; Yee, N.W.; Filip, S.V.; Hetrick, C.E.; Yang, B.; Green, W.H. Modeling Study of the Anti-Knock Tendency of Substituted Phenols as Additives: An Application of the Reaction Mechanism Generator (RMG). *Phys. Chem. Chem. Phys.* **2018**, *20*, 10637–10649. [[CrossRef](#)]
2. Mehl, M.; Vanhove, G.; Pitz, W.J.; Ranzi, E. Oxidation and Combustion of the N-Hexene Isomers: A Wide Range Kinetic Modeling Study. *Combust. Flame* **2008**, *155*, 756–772. [[CrossRef](#)]

3. Zhou, C.-W.; Li, Y.; O'Connor, E.; Somers, K.P.; Thion, S.; Keesee, C.; Mathieu, O.; Petersen, E.L.; DeVerter, T.A.; Oehlschlaeger, M.A.; et al. A Comprehensive Experimental and Modeling Study of Isobutene Oxidation. *Combust. Flame* **2016**, *167*, 353–379. [[CrossRef](#)]
4. Zhang, Y.; Somers, K.P.; Mehl, M.; Pitz, W.J.; Cracknell, R.F.; Curran, H.J. Probing the Antagonistic Effect of Toluene as a Component in Surrogate Fuel Models at Low Temperatures and High Pressures. A Case Study of Toluene/Dimethyl Ether Mixtures. *Proc. Combust. Inst.* **2017**, *36*, 413–421. [[CrossRef](#)]
5. Singaravelan, K.; Dhivakar, A.K.; Sivananth, M.; Vedharaj, S.; Balasubramanian, K.A. Effect of Oxygenated Additives on the Characteristics of a Diesel Engine. *Int. J. Appl. Eng. Res.* **2015**, *10*, 5.
6. Roubaud, A.; Lemaire, O.; Minetti, R.; Sochet, L.R. High Pressure Auto-Ignition and Oxidation Mechanisms of o-Xylene, o-Ethyltoluene, and n-Butylbenzene between 600 and 900 K. *Combust. Flame* **2000**, *123*, 561–571. [[CrossRef](#)]
7. Dussan, K.; Dooley, S.; Monaghan, R.F.D. A Model of the Chemical Composition and Pyrolysis Kinetics of Lignin. *Proc. Combust. Inst.* **2019**, *37*, 2697–2704. [[CrossRef](#)]
8. Font Palma, C. Model for Biomass Gasification Including Tar Formation and Evolution. *Energy Fuels* **2013**, *27*, 2693–2702. [[CrossRef](#)]
9. Weng, J.-J.; Tian, Z.-Y.; Liu, Y.-X.; Pan, Y.; Zhu, Y.-N. Investigation on the Co-Combustion Mechanism of Coal and Biomass on a Fixed-Bed Reactor with Advanced Mass Spectrometry. *Renew. Energy* **2020**, *149*, 1068–1076. [[CrossRef](#)]
10. Vanhove, G.; Petit, G.; Minetti, R. Experimental Study of the Kinetic Interactions in the Low-Temperature Autoignition of Hydrocarbon Binary Mixtures and a Surrogate Fuel. *Combust. Flame* **2006**, *145*, 521–532. [[CrossRef](#)]
11. Mergulhão, C.S.; Carstensen, H.-H.; Song, H.; Wagnon, S.W.; Pitz, W.J.; Vanhove, G. Probing the Antiknock Effect of Anisole through an Ignition, Speciation and Modeling Study of Its Blends with Isooctane. *Proc. Combust. Inst.* **2021**, *38*, 739–748. [[CrossRef](#)]
12. Song, H.; Dauphin, R.; Vanhove, G. A Kinetic Investigation on the Synergistic Low-Temperature Reactivity, Antagonistic RON Blending of High-Octane Fuels: Diisobutylene and Cyclopentane. *Combust. Flame* **2020**, *220*, 23–33. [[CrossRef](#)]
13. Fenard, Y.; Song, H.; Minwegen, H.; Parab, P.; Sampaio Mergulhão, C.; Vanhove, G.; Heufer, K.-A. 2,5-Dimethyltetrahydrofuran Combustion: Ignition Delay Times at High and Low Temperatures, Speciation Measurements and Detailed Kinetic Modeling. *Combust. Flame* **2019**, *203*, 341–351. [[CrossRef](#)]
14. Goldsborough, S.S.; Hochgreb, S.; Vanhove, G.; Wooldridge, M.S.; Curran, H.J.; Sung, C.-J. Advances in Rapid Compression Machine Studies of Low- and Intermediate-Temperature Autoignition Phenomena. *Prog. Energy Combust. Sci.* **2017**, *63*, 1–78. [[CrossRef](#)]
15. Goodwin, D.G.; Moffat, H.K.; Speth, R.L. *Cantera: An Object-Oriented Software Toolkit for Chemical Kinetics, Thermodynamics, and Transport Processes*; Caltech: Pasadena, CA, USA, 2018.
16. Fang, R.; Kukkadapu, G.; Wang, M.; Wagnon, S.W.; Zhang, K.; Mehl, M.; Westbrook, C.K.; Pitz, W.J.; Sung, C.-J. Fuel Molecular Structure Effect on Autoignition of Highly Branched Iso-Alkanes at Low-to-Intermediate Temperatures: Iso-Octane versus Iso-Dodecane. *Combust. Flame* **2020**, *214*, 152–166. [[CrossRef](#)]
17. Wagnon, S.W.; Thion, S.; Nilsson, E.J.K.; Mehl, M.; Serinyel, Z.; Zhang, K.; Dagaut, P.; Konnov, A.A.; Dayma, G.; Pitz, W.J. Experimental and Modeling Studies of a Biofuel Surrogate Compound: Laminar Burning Velocities and Jet-Stirred Reactor Measurements of Anisole. *Combust. Flame* **2018**, *189*, 325–336. [[CrossRef](#)]
18. Bounaceur, R.; Costa, I.D.; Fournet, R.; Billaud, F.; Battin-Leclerc, F. Experimental and Modeling Study of the Oxidation of Toluene. *Int. J. Chem. Kinet.* **2005**, *37*, 25–49. [[CrossRef](#)]
19. Emdee, J.L.; Brezinsky, K.; Glassman, I. A Kinetic Model for the Oxidation of Toluene near 1200 K. *J. Phys. Chem.* **1992**, *96*, 2151–2161. [[CrossRef](#)]
20. Lindstedt, R.P.; Maurice, L.Q. Detailed Kinetic Modelling of Toluene Combustion. *Combust. Sci. Technol.* **1996**, *120*, 119–167. [[CrossRef](#)]
21. Costa, I.D.; Fournet, R.; Billaud, F.; Battin-Leclerc, F. Experimental and Modeling Study of the Oxidation of Benzene. *Int. J. Chem. Kinet.* **2003**, *35*, 503–524. [[CrossRef](#)]
22. Luo, Y.-R. *Handbook of Bond Dissociation Energies in Organic Compounds*; CRC Press: Boca Raton, FL, USA, 2003; ISBN 0-8493-1589-1.
23. Davies, G.A.; Long, R. The Kinetics of the Thermal Hydrocracking of Cresols. *J. Appl. Chem.* **1965**, *15*, 117–127. [[CrossRef](#)]